

Evolution of Developmental Control Mechanisms

Grandparental stem cells in leech segmentation: Differences in CDC42 expression are correlated with an alternating pattern of blast cell fates

Shaobing O. Zhang^{a,1}, Dian-Han Kuo^b, David A. Weisblat^{b,*}^a Graduate Group in Biophysics, University of California, Berkeley, CA, USA^b Department of Molecular and Cell Biology, LSA 385, University of California, Berkeley, CA 94720-3200, USA

ARTICLE INFO

Article history:

Received for publication 17 March 2009

Revised 27 August 2009

Accepted 3 September 2009

Available online 9 September 2009

Keywords:

Segmentation

cdc42

Cell polarity

Leech

Asymmetric cell division

Grandparental stem cell

ABSTRACT

Embryonic segmentation in clitellate annelids (oligochaetes and leeches) is a cell lineage-driven process. Embryos of these worms generate a posterior growth zone consisting of 5 bilateral pairs of identified segmentation stem cells (teloblasts), each of which produces a column of segmental founder cells (blast cells). Each blast cell generates a lineage-specific clone via a stereotyped sequence of cell divisions, which are typically unequal both in terms of the relative size of the sister cells and in the progeny to which they give rise. In two of the five teloblast lineages, including the ventralmost, primary neurogenic (N) lineage, the blast cells adopt two different fates, designated nf and ns, in exact alternation within the blast cell column; this is termed a grandparental stem cell lineage. To lay groundwork for investigating unequal divisions in the leech *Helobdella*, we have surveyed the *Helobdella robusta* genome for genes encoding orthologs of the Rho family GTPases, including the *rho*, *rac* and *cdc42* sub-families, which are known to be involved in multiple processes involving cell polarization in other systems. We find that, in contrast to most other known systems the *Helobdella* genome contains two *cdc42* orthologs, one of which is expressed at higher levels in the ns blast cells than in nf blast cells. We also demonstrate that the asymmetric divisions of the primary nf and ns blast cells are regulated by the polarized distribution of the activated form of the Cdc42 protein, rather than by the overall level of expression. Our results provide the first molecular insights into the mechanisms of the grandparental stem cell lineages, a novel, yet evolutionarily ancient stem cell division pattern. Our results also provide an example in which asymmetries in the distribution of Cdc42 activity, rather than in the overall levels of Cdc42 protein, are important regulating unequal divisions in animal cells.

© 2009 Elsevier Inc. All rights reserved.

Introduction

In the embryos of clitellate annelids, including glossiphoniid leeches of the species *Helobdella*, segmental mesoderm and ectoderm arise by determinate lineages from a posterior growth zone (PGZ) consisting of five bilateral pairs of segmentation stem cells, the M, N, O/P, O/P and Q teloblasts (Fig. 1A). Columns of segmental founder cells called primary blast cells arise by the stem cell divisions of the teloblasts and coalesce, first ipsilaterally into left and right germinal bands and then along the ventral midline into a germinal plate. Developmental events in the segmentally iterated blast cell clones are indexed with reference to the clonal age (cl.ag.) at which they occur, i.e., the time elapsed since the birth of the primary blast cell that founded the clone in question. Morphologically recognizable segments arise from the extensive interdigitation of spatially

stereotyped clones, the composition of which varies according to the teloblast of origin (Weisblat and Shankland, 1985).

An intriguing feature of teloblastic segmentation processes seen in clitellates is that the N and Q teloblast lineages exhibit a grandparental mode of stem cell divisions. The concept of grandparental stem cell divisions originates in the analogy between cell lineage and human genealogical diagrams (Fig. 1B; Chalfie et al., 1981). In these lineages, the primary blast cells within each column adopt two distinct fates in exact alternation, as evidenced by the distribution and composition of the clones to which they give rise, starting with the timing and differential asymmetry of their first mitoses.

In the primary neurogenic (N) lineage, primary blast cells designated as nf divide at about 40 h cl.ag., the anterior daughter (nf.a) in the 2-cell clone is significantly larger than the posterior daughter (nf.p), and the definitive clone consists largely of neurons in the posterior lateral portion of one segmental ganglion and the anterior edge of the ganglion just behind it. In contrast, the intervening cells, designated ns, divide at about 44 h cl.ag., the anterior daughter (ns.a) in the 2-cell clone is only slightly larger than the posterior daughter (ns.p), and the clone consists largely of

* Corresponding author.

E-mail address: weisblat@berkeley.edu (D.A. Weisblat).¹ Present address: Stowers Institute for Medical Research, 1000 E. 50th St., Kansas City, MO 64110, USA.

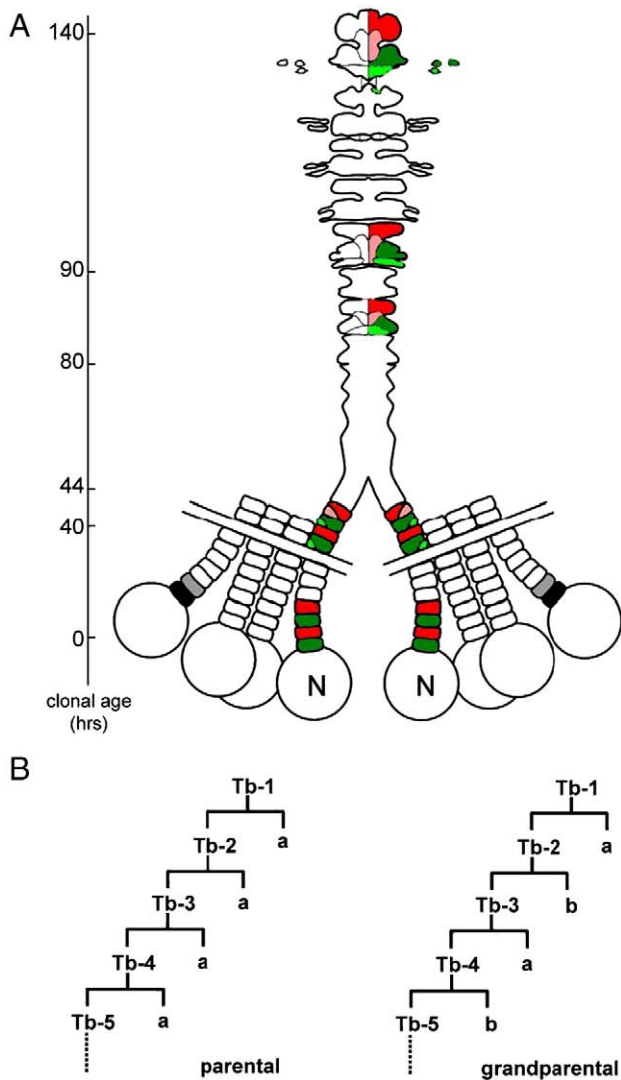


Fig. 1. Grandparental stem cell divisions in leech segmentation. (A) Asymmetric cell divisions in N teloblast lineage. Schematic depiction of cell lineage from the N teloblasts to segmental ganglia in *Helobdella*. The posterior growth zone comprises 4 pairs of ectodermal teloblasts (N is labeled) and 1 pair of mesodermal teloblasts (not shown). Each teloblast undergoes highly asymmetric divisions every 1.5 h, forming columns of segmental founder cells (primary blast cells) that coalesce first ipsilaterally and then along the ventral midline into the germinal plate, from which segmental tissues differentiate (only the ganglia are shown). Developmental events in primary blast cell clones can be timed in terms of “clonal age” (cl.ag., in hours on the scale at left), i.e., the time since the birth of the primary blast cell that founded the clone in question. In the N lineage, the primary blast cells comprise two types, ns (red) and nf (green) in exact alternation; ns and nf cells differ in terms of the timing (ns, 44 h cl.ag.; nf, 40 h cl.ag.) and extent (see Fig. 6) of their asymmetric, obliquely longitudinal first mitoses. These divisions yield ns.a/ns.p (red/pink) and nf.a/nf.p (green/light green) daughter cell pairs, which eventually contribute distinct sets of neurons to the differentiated ganglia (140 h cl.ag.). Anterior is up in all figures if not otherwise noted. (B) Cell lineage diagrams contrasting parental and grandparental stem cell divisions in the teloblast lineages. Each stem cell division gives a new generation of teloblast (Tb-x) and a segmental founder cell (a or b). In standard (parental) divisions, each generation of teloblast gives rise to the same type of blast cell; in grandparental divisions, odd numbered generations give rise to one type of blast cell (a) and even numbered generation give rise to another (b).

neurons in the medial and anterior lateral portion of a segmental ganglion (Fig. 1A; Zackson, 1984; Bissen and Weisblat, 1987).

The overall size differences between the nf and ns daughter cell pairs are accompanied by differences in nuclear size (Zackson, 1984). More recent work, involving 3-D reconstructions of pairs of nuclei prepared from stacks of confocal images, revealed that the nuclear

volume ratios of the daughter cell pairs resulting from the mitosis of nf and ns blast cells are clearly distinct and show little variance (Zhang and Weisblat, 2005). The tightly regulated asymmetry of the nf and ns mitoses entails first a rotation of the mitotic apparatus and then its rearward shift relative to the cell cortex during anaphase. The rearward shift of the mitotic apparatus is greater in nf cells than in ns cells, which accounts for the differential asymmetry in the nf and ns divisions (Zhang and Weisblat, 2005).

In the budding yeast *Saccharomyces cerevisiae*, Cdc42, a Rho family small GTPase, is preferentially localized to and activated at the cell cortex at the prospective bud site (Ziman et al., 1993; Toenjes et al., 1999; Richman et al., 2002). This asymmetric distribution of Cdc42 activity is required for the formation of two daughter cells of different sizes and fates (Toenjes et al., 1999). Thus, the work presented here was initiated to test for the involvement of a *cdc42*-class gene in the unequal mitoses of nf and ns blast cells. Along with Rac- and Rho-class proteins, Cdc42 and its homologs make up the Rho family of the Ras superfamily of small GTPases (Takai et al., 2001; Boureux et al., 2007). As such, Cdc42 cycles between an activated GTP-bound state and an inactivated GDP-bound state, and has been implicated in the regulation of cell polarity and unequal cell divisions in yeast and multicellular organisms (reviewed in Etienne-Manneville and Hall, 2002). We sought to characterize the *Helobdella cdc42* gene to ask if differences in its expression, localization and/or activity control the differentially asymmetric mitoses in ns and nf blast cells.

We find two *cdc42* homologs in *Helobdella*, one of which is expressed at higher levels in the ns than in nf blast cells, as judged by *in situ* hybridization and by staining for CDC42-like immunoreactivity. This difference provides an early molecular marker for the alternating nf and ns fates in *Helobdella*. The difference in transcript levels is evident at very early clonal ages, many hours before the n blast cells undertake their first mitoses and before the appearance of CDC42-like immunoreactivity. Over-expressing the wildtype Cdc42 homolog itself did not affect the asymmetry of the n blast cell mitoses. Instead, we show that the asymmetric divisions of these cells are regulated by the polarized distribution of the activated form of the protein, rather than by the overall level of expression. These results provide the first molecular insights into the mechanisms of a novel, yet evolutionarily ancient stem cell division pattern and also provide an example of asymmetrically distributed Cdc42 activity in asymmetrically dividing animal cells.

Materials and methods

Embryos

Embryos were obtained from an as yet unnamed *Helobdella* species collected in Austin (Texas, USA) and provisionally referred to here as *Helobdella* sp. (Austin) (Hau; M. Shankland, personal communication). *Hau* is closely related to *Helobdella robusta* (Hro; Shankland et al., 1992; Bely and Weisblat, 2006), and until recently (Bely and Weisblat, 2006) has been regarded as a variant of that species (Zhang and Weisblat, 2005; Agee et al., 2006; Ren and Weisblat, 2006; Seaver and Shankland, 2000, 2001; Kuo and Shankland, 2004). Embryos of *Hau* were used in this work because this species is more readily cultured in the laboratory. Developmental progress is indicated according to a staging system applicable to all glossiphoniid leeches (Weisblat and Huang, 2001) or, for greater precision, in terms of the time after zygote deposition (AZD).

Molecular sequence analysis

Sequences for Rac/CDC42 small GTPases in human (Hsa), *Drosophila melanogaster* (Dme) and *Caenorhabditis elegans* (Cel) were recovered from NCBI database and were confirmed by reciprocal BLAST searches.

Accession numbers: CAB53579.5 (Hsa-rac1); CAG30441.1 (Hsa-rac2); AAC51667.1 (Hsa-rac3); NP_001782.1 (Hsa-CDC42 isoform1); NP_476950.1 (Dme-rac1); NP_648121.1 (Dme-rac2); AAD43792.1 (Dme-CDC42); NP_524533.1 (Dme-MTL); NP_500363.1 (Cel-Rac1/CED10); NP_001040961.1 (Cel-Rac2); NP_495598.1 (Cel-CDC42); NP_509931.1 (Cel-Mig2). Gene models for members of Rho family in *H. robusta*, *Capitella* sp. I, and *Lottia gigantea* were recovered by BLAST search against whole-genome assemblies produced by the Joint Genome Institute (DOE). The recovered amino acid sequences were aligned using ClustalX 2.0 (Larkin et al., 2007). Neighborhood-joining (NJ) and Maximum-Likelihood (ML) trees were built using MEGA 4 (Tamura et al., 2007) and PHYML (Guindon et al., 2005) respectively. Bootstrap was performed with 1,000 and 500 repeats for NJ and ML trees respectively.

Molecular cloning and mRNA injection

Prior to the availability of the whole genome data, degenerate PCR primers (forward: GGNGCNGTNGGIAARACITG, cognate amino acid sequence: 12GAVGKTC18; reverse: MTCYCYTGNGGIGCIGTRTC, 57DTAGQED63) were designed to cover conserved Cdc42 protein N-terminal sequence. *Hro-cdc42a* cDNA was obtained from a cDNA library (Stratagene) prepared from stage 1 - stage 6 *H. robusta* embryos. Sequence specific primers (3': CCATCYGAATATGTSCTAC; 5': GTAGGSACATATTCRGATGG) were used to perform 3' and 5' rapid amplification of cDNA ends (RACE) to get full-length cDNA sequence. Identical cDNA sequences were amplified from *Hro* and *Hau*.

Helobdella cdc42b, *rac1*, and *rac2* were first identified from the *Hro* whole genome assembly (Joint Genome Institute, DOE). cDNA fragments containing the complete coding region and partial 3'UTR of *cdc42a*, *cdc42b*, *rac1*, and *rac2* were PCR amplified from embryonic cDNA of both species. PCR primers were designed based on the sequence information obtained from the genome assembly (*cdc42a* forward: CCTCGTCTATTAAATTCCTC; *cdc42a* reverse: GACTTTCATTGGGAATA-TATGCACAAAAATACCCAAACT; *cdc42b* forward: ATGCAGACGAT-TAAATGTGTC; *cdc42b* reverse: GTATCTATGGCTGTGTAGTACTACT; *Rac1* forward: ATGCAGGCCATAAAGTGTGTCGTT; *Rac1* reverse: TAGGACTTCTGCATTCTCTCAATG; *Rac2* forward: ATGCAAGCTATAAAA-TGTGTCGTG; *Rac2* reverse: GTTCAACGGGGTCGTTCACTACTA). The amplified DNA fragments were gel extracted and cloned into pGEM-T Easy (Promega). These plasmids were designated as pHau-CDC42A (GQ892926), pHau-CDC42B (GQ892927), pHau-Rac1 (GQ892928), and pHau-Rac2 (GQ892929), respectively.

To build an expression construct, the coding sequence of Hau-CDC42A was PCR amplified with primers designed to add an *EcoRI* site and a linker region (Alanine₈) at the N terminal and a *PstI* site at the C terminal. YFP cDNA was PCR amplified as a fragment flanked by *BamHI* and *EcoRI* sites. YFP and Hau-CDC42A fragments were fused (YFP::EFA₈::Hau-CDC42A) and cloned into pCS2p vector using *BamHI* and *PstI* sites. Mutagenic PCR primers were used to make G12V, Q61L and T17N mutant CDC42 constructs from pCS2p-YFP::Hau-CDC42A plasmid, using the QuickChange site-directed mutagenesis kit (Stratagene). Constructs were linearized with *NotI* and transcribed *in vitro* using mMessage mMachine Sp6 kit (Ambion). mRNA, plasmid, and rhodamine-conjugated lysine dextran lineage tracer (RDA; Gimlich and Braun, 1985) were injected as previously reported (Zhang and Weisblat, 2005). In short, by injecting an N teloblast at the onset of stage 7 (33 h AZD), the first targeted primary blast cell is the ns blast cell contributing its progeny to segmental ganglion R4. Unless otherwise noted, the concentrations of mRNAs injected were 0.4 µg/µl in the needle (roughly 4 ng/µl in the N teloblast).

Semi-quantitative RT-PCR (sqRT-PCR)

sqRT-PCR was performed as previously described (Song et al., 2002).

In situ hybridization and immunostaining

For *in situ* hybridization, digoxigenin labeled antisense probes were transcribed *in vitro* using MEGAScript T7 or SP6 kits (Ambion). Probe for *Hro-cdc42a* coding region was transcribed from linearized pCS2p-YFP::HRO-CDC42A template, and an alternative probe that covers the coding region and part of 3' UTR was transcribed from linearized pHro-CDC42A. Probes for *Hro-cdc42b*, *Hro-rac1*, and *Hro-rac2* were transcribed from linearized pHro-CDC42B, pHro-Rac1, and pHro-Rac2 respectively. *In situ* hybridization experiments were performed as described previously (Song et al., 2002). For immunostaining, primary goat polyclonal anti-CDC42 (cN-17) (#sc-9279, Santa Cruz Biotechnology) was used at 1:1000 dilution. Horseradish peroxidase (HRP) conjugated secondary antibody was from Santa Cruz Biotechnology (#sc-3851). Immunostaining was carried out as described previously (Goldstein et al., 2001).

Imaging

YFP::HRO-CDC42 fluorescence time-lapse image stacks were acquired (1-min interval; 5 µm steps) on a Nikon E800 epifluorescence microscope equipped with a cooled CCD camera (Princeton Instruments), controlled by Metamorph software (UIC). Image stacks were processed with Metamorph and/or ImageJ (NIH) to prepare the snapshots and movies presented in this paper. Images of nuclear GFP (nGFP, i.e., GFP targeted to the nucleus by inclusion of a nuclear localization signal) were acquired under a Zeiss 510 Axioplan confocal microscope. Confocal images were processed and nuclear volumes were measured in Volocity 3.0 (Improvision). All exported images were processed with Photoshop 5.0 (Adobe).

Results

Duplicate *rac* and *cdc42* genes in the *Helobdella* genome

In Metazoa, Rho family small GTPases are divided into six subfamilies, including Rac, CDC42, MTL, Rho, RhoU and RhoBTB (Boureaux et al., 2007). There are 11 putative Rho family small GTPase genes in the annotated *H. robusta* genome, including two *rac* orthologs and surprisingly, two *cdc42* orthologs (Fig. 2). Among other animals that have been surveyed, *cdc42* gene duplications have been observed in various deuterostomes (hemichordate, teleost fish, and opossum), but not in other vertebrates, echinoderms or ascidians, nor in any of other taxa including cnidarian, sponge, fluke, nematode or fly (Boureaux et al., 2007). The other seven genes encode one *mtl* ortholog, three putative *rho* orthologs, two *rhoU* orthologs and one *rhoBTB* ortholog. We were able to clone and sequence the *rac* and *cdc42* orthologs from both *H. robusta* and from *H. sp.* (Austin) cDNAs, thereby confirming their identity. We have therefore designated these eight genes as *Hro-* and *Hau-rac1*, *-rac2*, *-cdc42a* and *-cdc42b*. The *cdc42a* cDNA sequences in *Hau* and *Hro* were identical at the nucleotide level, as were their respective *cdc42b* sequences.

The amino acid sequences of the hypothetical *Helobdella* CDC42A and CDC42B proteins are 90% identical overall, and align closely with those of other metazoans and yeast (Fig. 2). In particular, their N terminal 84 amino acids are identical to those of the *C. elegans* protein, and it was the N terminal sequence of the *C. elegans* protein that was used to generate the commercial polyclonal antibody used here. Similarly, *Hro-RAC1* and *Hro-RAC2* are 95% identical between themselves, 69–71% identical overall in pairwise combination with the *Hro-CDC42* proteins, and 81% identical to the *Hro-CDC42* proteins in the N terminal region, with primarily conservative substitutions. The extensive similarities between the two *rac* genes and between the two *cdc42* genes in *Helobdella* suggest that they may represent fairly recent gene duplication events. This interpretation is supported by the fact that we found no evidence for

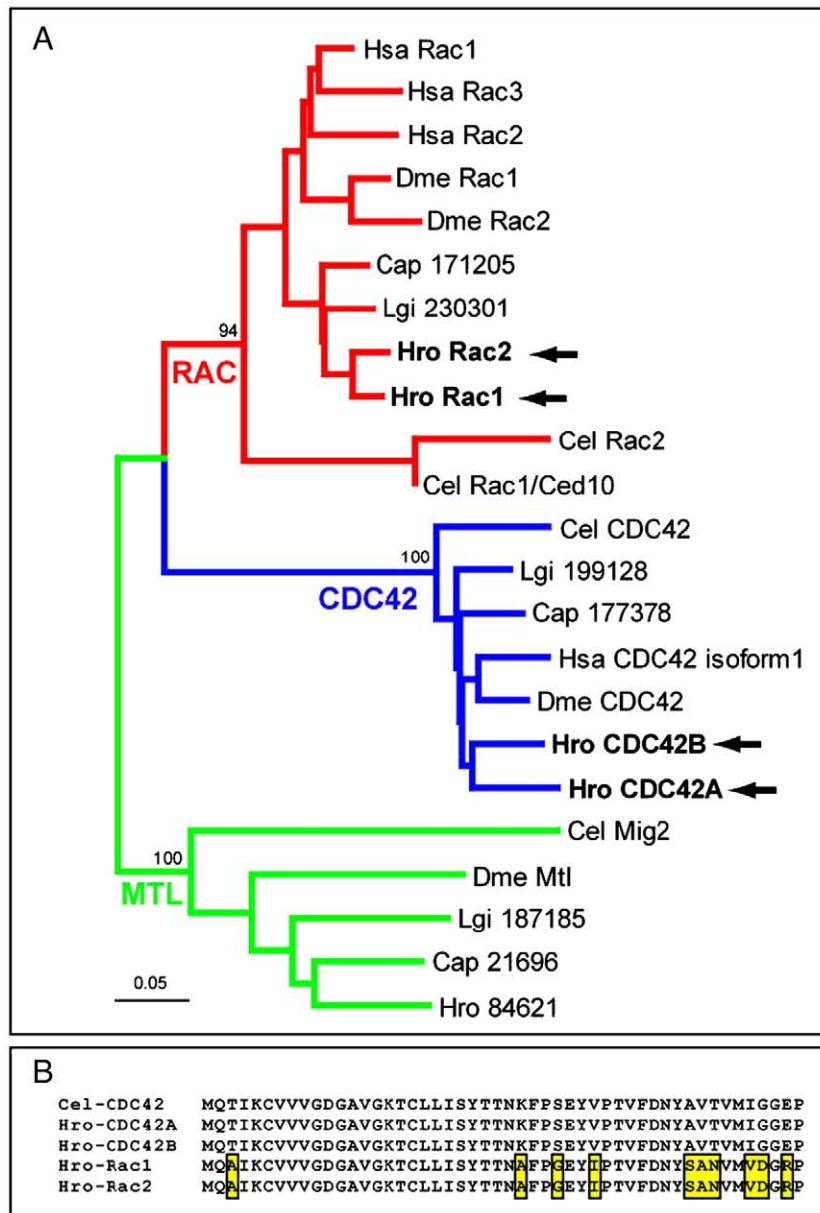


Fig. 2. Molecular sequence analysis of *Helobdella* Rac/CDC42 small GTPases. (A) Unrooted NJ tree of Rac/CDC42 small GTPases from five representative metazoan species. Bootstrap analysis (1000 repeats) shows well-supported Rac (red), CDC42 (blue) and MTL (green) clusters. ML trees show a similar topology (not shown). The *Helobdella* genes that are further isolated and studied here are indicated by bold type and arrows. Amino acid sequences for all genes from *Capitella* sp. 1 (a polychaete worm) and *Lottia gigantea* (a limpet) and the *Helobdella* MTL homolog were recovered from JGI gene model collections. Gene model protein ID numbers assigned by JGI are used instead of generic names for these unconfirmed gene models. Abbreviated species names: Hsa (*Homo sapiens*), Dme (*Drosophila melanogaster*), Cel (*Caenorhabditis elegans*); Cap (*Capitella* sp. 1); Lgi (*Lottia gigantea*); Hro (*Helobdella robusta*). (B) The first 50 N terminal amino acid residues of Cel-CDC42 align with the four *Helobdella* Rac/CDC42 proteins. The amino acids in this region were completely identical between the CDC42 proteins. Only ten different amino acid changes were identified between CDC42 and Rac proteins (yellow boxes).

duplication of either *rac* or *cdc42* genes in two other lophotrochozoan genomes, (*Capitella* sp. 1 and *Lottia gigantea*). To examine the expression and function of these Rho GTPases in the unequal blast cell divisions, we focused on the embryos of *H. sp.* (Austin), which is more readily maintained in laboratory culture.

Within the N teloblast lineage, Hau-cdc42a is expressed preferentially in ns blast cells

Given the extensive conservation of amino acid sequences among the four *Helobdella* RAC and CDC42 peptide sequences, immunostaining is not expected to distinguish between these four proteins. At the nucleotide level, however, the two *cdc42* homologs differ substantially from the two *rac* homologs (maximum 68% identity between

Hau-cdc42a and *Hau-rac1*), and *Hau-cdc42a* and *Hau-cdc42b* are only 76% identical overall. Thus, we anticipated that *in situ* hybridization should permit us to distinguish the expression of these genes during stages 7–8, during which the blast cells arise from the asymmetric cell divisions of the teloblasts.

Semi-quantitative RT-PCR (sqRT-PCR) analysis (Figs. 3A, B) revealed that *Hau-cdc42a* transcript is in higher abundance than *Hau-cdc42b* until late in development, but its level fluctuates over the course of development. The *Hau-cdc42b* transcript is present in early cleavage stages and in late development, but is almost undetectable during stages 6–8. *Hau-cdc42b* amplicon was not clearly visible at most stages until after 33 rounds of PCR amplification whereas *Hau-cdc42a* was readily detectable at 28 cycles (Fig. 3A). Hence, our sqRT-PCR data suggested that, of these two genes, *Hau-cdc42a* is more likely

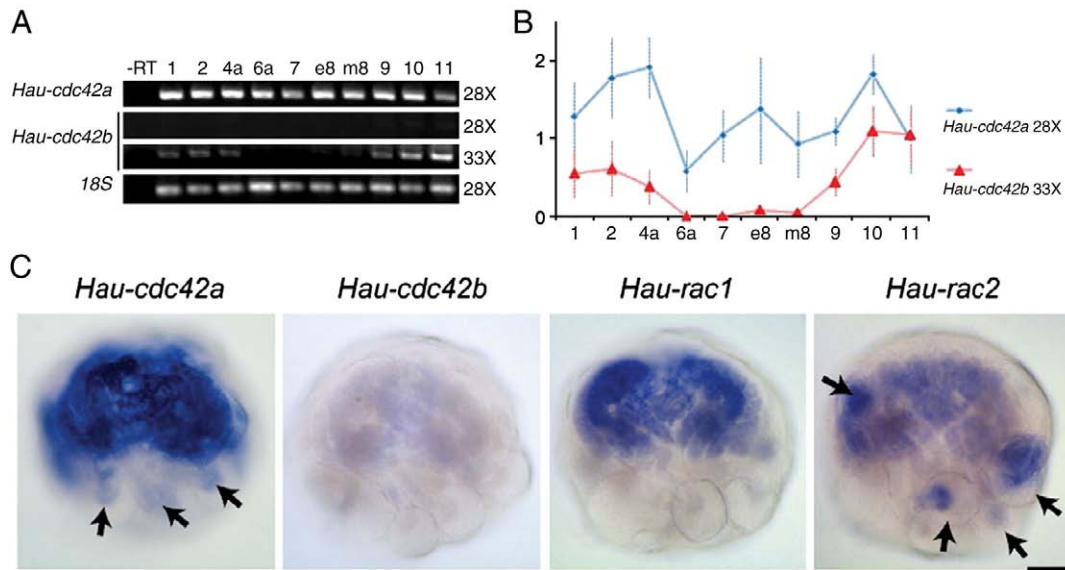


Fig. 3. Expression of the *Helobdella cdc42* and *rac* genes. (A, B) sqRT-PCR reveals distinct temporal dynamics of *Hau-cdc42a* and *Hau-cdc42b* expression. (A) For *Hau-cdc42a*, a clear band was observed for every developmental stage after 28 cycles of amplification (A, row 1); normalizing relative to 18S revealed that *Hau-cdc42a* is relatively abundant, and that its levels fluctuate within a four fold range over the course of embryonic development (B). In contrast, the *Hau-cdc42b* amplicon was barely detectable after 28 amplification cycles (A, row 2), and only became readily visible with five additional cycles (A, row 3). *Hau-cdc42b* declines to very low levels in stages 6 through mid 8, and increases in later stages (B). (C) *In situ* hybridization of embryos at early stage 8 is consistent with sqRT-PCR data; *Hau-cdc42a* transcripts are evident in the germinal bands and to a lesser extent in the teloblasts (arrows) while probe for *Hau-cdc42b* gives essentially no staining. Under identical conditions *Hau-rac1* shows expression in the germinal bands at lower levels than *Hau-cdc42a* while *Hau-rac2* transcripts are seen primarily in teloblasts (arrows). Scale bar, 80 microns.

to be involved in the phase of segmentation represented by the production and unequal early divisions of the blast cells.

In situ hybridization experiments were consistent with the sqRT-PCR results. In stage 7–8 embryos, *Hau-cdc42a* probes yielded strong staining in the germinal bands and fainter but detectable staining of teloblasts under conditions where *Hau-cdc42b* probes of similar length and concentration gave no staining above background (Fig. 3C). Parallel *in situ* hybridization reactions revealed that *Hau-rac1* and *Hau-rac2* are present in somewhat complementary distributions; *Hau-rac1* is present in the germinal bands, but not in teloblasts, while *Hau-rac2* is more evident in teloblasts than in germinal bands. Probes for all three genes, *Hau-cdc42a*, *Hau-rac1* and *Hau-rac2* also stained cells between the germinal bands in an area known as the micromere cap (Fig. 3C). The broad expression of these genes is in keeping with their many roles in cells.

Careful inspection of embryos stained for *Hau-cdc42a* revealed that *Hau-cdc42a* mRNA is more abundant in ns than in nf cells (Fig. 4A). Moreover, the alternating *Hro-cdc42a* levels in ns and nf blast cells were evident by ~6 h clonal age (Fig. 4A). In n blast cells younger than ~6 h clonal age, the pattern of *Hro-cdc42a* expression was variable and adjacent cells often contained similar levels of *Hro-cdc42a* (Fig. 4A). This observation suggests that at least some aspects of ns and nf blast cell identity arise after the primary blast cells are born from the N teloblast. We did not observe an alternating staining pattern for *Hau-cdc42b*, *Hau-rac1* or *Hau-rac2*. Thus, subsequent analyses focused on *Hau-cdc42a*.

Immunostaining suggests that Hau-CDC42A protein is also elevated in ns blast cells

As discussed above, immunostaining with the commercially available antibody, raised to the highly conserved N terminal portion of the CDC42 ortholog from *C. elegans*, cannot give conclusive evidence that the observed *Hau-cdc42a* mRNA is being translated, because this antibody is not expected to distinguish Hau-CDC42A from Hau-CDC42B, Hau-RAC1, Hau-RAC2 and possibly other Rho GTPases. Consistent with this prediction, we found the antibody recognizes a protein band of the appropriate molecular weight for

CDC42 and Rac proteins (about 21 kDa) in embryonic western blots (Fig. 5A). This band is present at all stages examined, as is another band of about equal intensity in the range of 70 to 80 kDa. We speculate that this higher MW band may correspond to the RhoBTB family member.

In a second test of the antibody, we injected individual teloblasts (stage 7) with *yfp::Hau-cdc42a* mRNA transcribed *in vitro*. Immunostaining the injected embryos 2 days later revealed preferential staining of the column of blast cells arising from the injected teloblast (Figs. 5B, C), as well as a general staining of the embryo that we attribute to endogenous Rho GTPases.

Together these results indicate that the available antibody does recognize Hau-CDC42 in the embryo, and presumably other Rho GTPases. Thus, in conjunction with the *in situ* results, which suggest differential expression between nf and ns blast cells only for *Hau-cdc42a*, the onset of CDC42-like immunoreactivity in the n bandlet

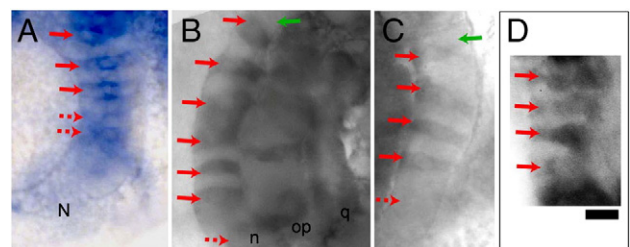


Fig. 4. Differential expression of *Hau-cdc42a* in nf and ns blast cells. (A) *In situ* hybridization showing the portion of n bandlet proximal to the N teloblast in stage 7 embryos. (A) Alternating pattern of *Hro-cdc42a* mRNA levels, elevated in ns cells (red arrows) is evident soon (~7 h cl.ag.) after the n blast cells are born; younger ns cells (dashed red arrows) that do not show elevated *Hro-cdc42a* levels lie closer to the parent teloblast (N). Black arrow points to an nf which is the latest born. (B, C) Examples of left (B) and right (C) N lineages in early stage 8 embryos show that CDC42-like immunoreactivity is higher in premitotic ns cells (red arrows) than in the intervening nf cells. The oldest ns cell that has not yet upregulated CDC42-like immunoreactivity (dashed red arrows, ~26 h cl.ag.) and the most recently divided nf cell (green arrows, ~40 h cl.ag.) are indicated in each sample. (D) The same pattern of elevated immunoreactivity in ns blast cells (red arrows) is seen in cells destined for posterior segments in embryos fixed and stained at mid stage 8. Scale bar, 10 microns.

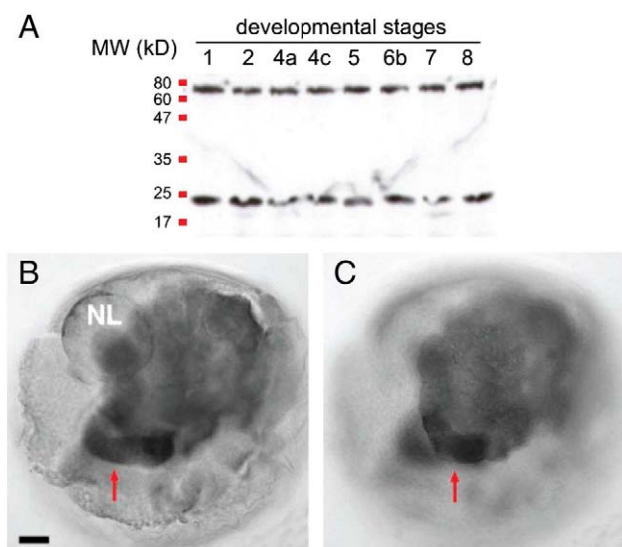


Fig. 5. Immunostaining for Hau-CDC42A. (A) Western blot analysis of *Helobdella* embryos with commercial CDC42 antibody detects two prominent bands at all stages of development, one at about 21 kDa, corresponding to the predicted MW of the Hau-CDC42A, Hau-CDC42B, Hau-RAC1 and Hau-RAC2; see Fig. 2B) and another between 60 and 80 kDa, which does not correlate with any known Rho GTPase from the genome. Minor bands are visible at stages 2 and 7. (B, C) Deep (B) and superficial (C) focal planes of an embryo in which the left N teloblast (NL) was injected with synthetic *Hau-cdc42a* mRNA. The embryo injected embryo was fixed and immunostained with the cross-reactive antibody roughly 2 days later. The n bandlet (arrow) derived from the injected teloblast stains more strongly, indicating that the antibody recognizes Hau-CDC42A. Scale bar, 50 microns.

should permit us to infer the **earliest** point at which Hau-CDC42A protein might be accumulating in cells of interest.

With these caveats in mind, we examined the pattern of immunostaining in the n bandlets of normal embryos. Immunostaining was seen at uniformly low levels in all primary blast cells proximal to the teloblast, but increased specifically in ns cells that were older than about 26 h cl.ag. As a result, protein levels alternated (higher in ns cells and lower in nf cells) beginning with undivided (primary) blast cells (26 h cl.ag.) and continued at least through their first mitoses (roughly 44 h cl.ag.; Figs. 4B, C). These observations were made on embryos fixed at early stage 8 (roughly 96 h AZD). We also observed the pattern of elevated CDC42-like immunoreactivity in undivided n blast cells of embryos fixed at mid stage 8 older absolute ages (roughly 120 h AZD, Fig. 4D), indicating that this pattern does not result from segment-specific differences in expression, but instead represents a consistent difference between the nf and ns blast cells, corresponding to the observed difference in *Hau-cdc42a* transcript levels.

Thus, while the cross-reactivity of the antibody means that we cannot be sure that the observed immunostaining represents Hau-CDC42 protein, our results are consistent with the hypothesis that this pattern reflects the accumulation of Hau-CDC42A in ns blast cells starting at approximately 26 h cl.ag., i.e., with a delay of about 20 h after the appearance of *Hau-cdc42a* mRNA. Together, the *in situ* and immunostaining results suggest that differences in *Hau-cdc42a* transcription, transcript processing and/or stability between the ns and nf blast cells result in corresponding differences in Hau-CDC42A protein levels, and that the mRNA differences are present as a pre-pattern in the n bandlet.

Posteriorly localized CDC42A activity regulates asymmetric divisions of nf and ns cells

Injecting N teloblasts with *yfp::Hau-cdc42a* mRNA resulted in the expression of YFP::Hau-CDC42A protein at high levels compared to

the native protein as judged by immunostaining (Figs. 5B, C), yet this had no obvious effects on the production of n blast cells by the teloblast (Figs. 5B, C). To look more carefully for functional consequences of what appears to be quantitative differences in Hau-CDC42A expression between ns and nf blast cells, we looked for changes in n blast cell division patterns resulting from the expression of YFP::Hau-CDC42A. For this purpose, N teloblasts were injected with a mixture of *yfp::Hau-cdc42a* and *ngfp* mRNAs to visualize the YFP::Hau-CDC42A protein distribution in living cells, and the nuclei of fixed cells inheriting the injected mRNAs, respectively. Injections were uniformly carried out at early stage 7 (about 33 h AZD) and the injected embryos were observed at early stage 8, roughly 2 days after injection.

A priori, we anticipated that nf cells with elevated Hau-CDC42A levels might divide more like ns cells (i.e., later and/or less asymmetrically) but no such defects were observed. In all embryos ($n = 74$) injected with a mixture of *yfp::Hau-cdc42a* and *ngfp* mRNAs, the ns and nf blast cells exhibited their normal, differentially asymmetric cell divisions (Fig. 6A; compare with Fig. 7 of Zhang and Weisblat, 2005), as did the injected teloblasts (not shown). The nuclear volume ratios calculated for the products of both nf and ns blast cell divisions (Fig. 6A) were all within the range of previously measured values ($V_{ns,p}/V_{ns,a} = 0.51 \pm 0.05$ and $V_{nf,p}/V_{nf,a} = 0.23 \pm 0.03$; Zhang and Weisblat, 2005).

We have shown previously that injecting teloblasts with mRNA yields a gradient of protein expression within the descendant blast cells: blast cells born soon after the injection express low levels of the protein, while those born later inherit progressively higher levels from the injected teloblast (Zhang and Weisblat, 2005). This was also true for the YFP fusion proteins expressed in our present experiments (data not shown), but ns and nf blast cells corresponding to all axial positions in YFP::Hau-CDC42A-expressing embryos divided normally.

Imaging live embryos revealed that YFP::Hau-CDC42A was localized to the cortical cytoplasm of n blast cells in interphase and mitosis. In contrast to the situation in budding yeast (Richman et al., 2002), this fusion protein did not show an asymmetric distribution between the anterior and posterior cortices in either nf or ns blast cells ($n = 16$) (Figs. 7A, B).

As a Rho family GTPase, Cdc42 cycles between an active GTP-bound form and an inactive GDP-bound form, and the proportion of the overall Cdc42 protein in these two forms is under kinetic control of guanine nucleotide exchange factors, GTPase-activating proteins and GDP-dissociation inhibitors (Hall, 2005). Thus, changing overall Cdc42 protein levels in the experiment described above may not have affected the levels of activated Cdc42. To affect levels of active Hau-CDC42A directly, and follow the distribution of the activated, GTP-bound form of Hau-CDC42A, we co-injected N teloblasts with a mixture of *ngfp* mRNA and mRNA encoding YFP fused to Hau-CDC42A^{G12V} or Hau-CDC42A^{Q61L}. These mutant proteins cannot efficiently hydrolyze bound GTP and thus are trapped in the active form (Hall, 2005; Hutterer et al., 2004). Identical results were obtained with both constructs. Thus, for simplicity they are designated hereinafter as YFP::Hau-CDCA42^{G12V/Q61L}.

In accord with the expected gradient of protein expression in blast cells after injecting the teloblast with mRNA, the first few blast cells born after the *yfp::Hau-cdc42a*^{G12V/Q61L} mRNA injection (up to 7 blast cells in a single N teloblast lineage) expressed YFP::Hau-CDC42A^{G12V/Q61L} at tracer levels. That is to say, these cells exhibited relatively low YFP fluorescence and the ns and nf cells divided with normal timing and asymmetry, so the mutant protein was evidently not present in levels sufficient to disrupt normal cell division pattern. Consistent with our previous findings, the nf blast cell divisions were markedly unequal with nuclear volume ratios ($V_{nf,p}/V_{nf,a}$) of about 0.25; ns blast cell divisions were also unequal but less so, with nuclear volume ratios ($V_{ns,p}/V_{ns,a}$) of about 0.5 (Figs. 6B, C). These volume ratios are within

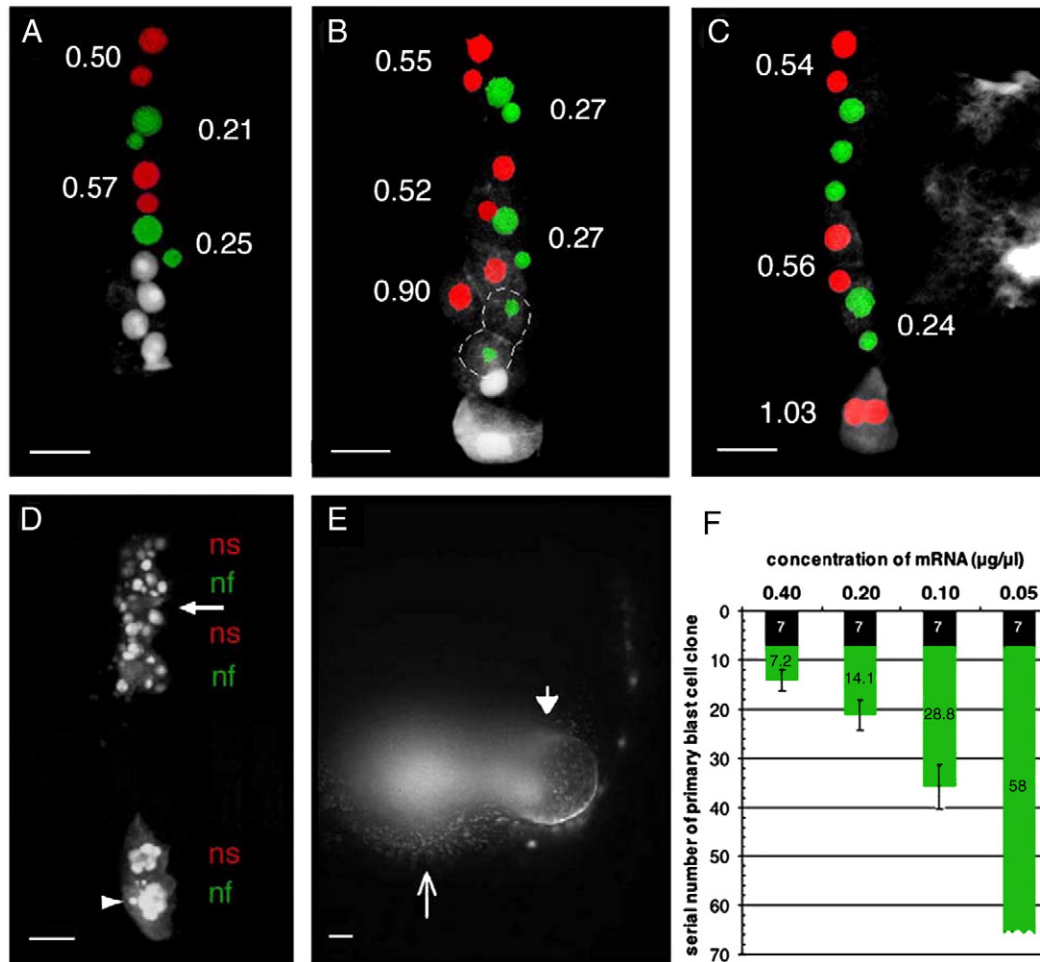


Fig. 6. Expression of constitutively active Hau-CDC42A above threshold level equalizes the nf and ns blast cell divisions. (A–C) Nuclear volume ratios were obtained ($V_{\text{post. cell}}/V_{\text{ant. cell}}$; see text for details) for daughter cell pairs arising from the mitoses of ns and nf blast cells (red and green, respectively). Nuclei of undivided, primary blast cells are shown in white. (A) Over-expression of YFP::Hau-CDC42A does not affect the differentially asymmetric ns and nf blast cell mitoses (quantified as described in text); nuclear volume ratios are indistinguishable from previous measurements (Zhang and Weisblat, 2005) and the injected lineages developed normally (not shown). (B–D) Over-expression of YFP::Hau-CDC42A^{G12V/Q61L} equalizes both ns and nf divisions, as judged by nuclear ratios (B, C) and by cell sizes (B, dashed outlines), but only in blast cells arising several cell cycles after injection of the parent N teloblast. [In (C), the anteriormost nf clone has undergone a normal second mitosis, so the nf.p/nf.a nuclear volume ratio could not be determined for that clone.] Orientations of divisions in affected blast cells appear to be randomized [e.g., posteriormost ns mitosis in (C)]. (D) After 2 days of subsequent development, clones of ns and nf with normal first divisions appear to develop normally, as evidenced by overall clone morphology, further asymmetric divisions (note range of nuclear sizes in 4 anterior clones) and the formation of intersegmental segmental fissures between such clones (arrow). In contrast, clones of affected n blast cells develop abnormally, with fewer and equal mitoses, often associated with their separation from the anterior portions of the bandlet. Here, the two posterior clones contain only 5–6 cells each. The posterior clone also shows what appear to be nuclear fragments indicative of dying cells (arrowhead). Such clones cannot be distinguished as nf or ns by their morphology and the assignments indicated here are based on their sequence relative to the anterior portion of the n bandlet. (E) Some time after the transition to producing blast cells that undergo equal mitoses, the injected N teloblast itself has undergone a roughly equal division (progeny indicated by arrow and arrowhead). After one or two such divisions, the affected teloblasts cease dividing. (F) The transition from normal to equalized n blast cells after the injection of N teloblast with *Hau-cdc42a*^{G12V/Q61L} mRNA is dose dependent. Teloblasts were injected after seven n blast cells had been produced (black bar) and the number of n blast cells undergoing normal, differentially asymmetric division after injection was determined (green bar). At the lowest concentration, (0.05 μg/μl) no transition from normal to equalized mitoses was observed (denoted by jagged bar end). Scale bar, 20 microns.

the range of those measured for control blast cells and for blast cells over-expressing wild-type Hau-CDC42A. In such cells, (11/12), YFP::Hau-CDC42A^{G12V/Q61L} localized preferentially to the posterior cortices and was segregated to the posterior (smaller) daughters of both blast cell types (Figs. 7C–F), in clear distinction to the wild-type protein.

In contrast to the first few n blast cells born after N teloblasts were injected with *yfp::Hau-cdc42a*^{G12V/Q61L}, those born later exhibited higher levels of YFP fluorescence, reflecting higher levels of the translated mutant protein. Strikingly, these cells appeared to divide equally, and with unpredictable, apparently randomized spindle orientation, in 68 of 72 embryos (94%). Moreover, although the increase in YFP::Hau-CDC42A^{G12V/Q61L} levels was presumably gradual, the transition from normal to abnormal divisions was abrupt, occurring between one blast cell and the next (Figs. 6B, C). Quantification of the change in division pattern was obtained as

before, by reconstructing sister cell nuclei from stacks of confocal images obtained from embryos fixed at a point where they contained 2-cell clones of both normal, asymmetric and abnormal, equalized n blast cell divisions (Figs. 6B, C). Consistent with the qualitative observations, the measured nuclear volume ratios changed from normally asymmetric divisions to nuclear volume ratios that were not significantly different from unity (nuclear ratios of 0.95 ± 0.04 , $n = 8$ including both nf and ns divisions).

Despite the disruption of the normal asymmetry and orientation of mitosis in n blast cells resulting from elevated levels of constitutively active YFP::Hau-CDC42A^{G12V/Q61L}, the nominal ns and nf cells divided at their normal clonal ages of 44 h and 40 h, respectively. Together, these observations suggest that the cell cycle duration is controlled independently of the position and orientation of the mitotic apparatus, and that only these two latter aspects of the blast cell division are regulated by the polarized distribution of activated CDC42A.

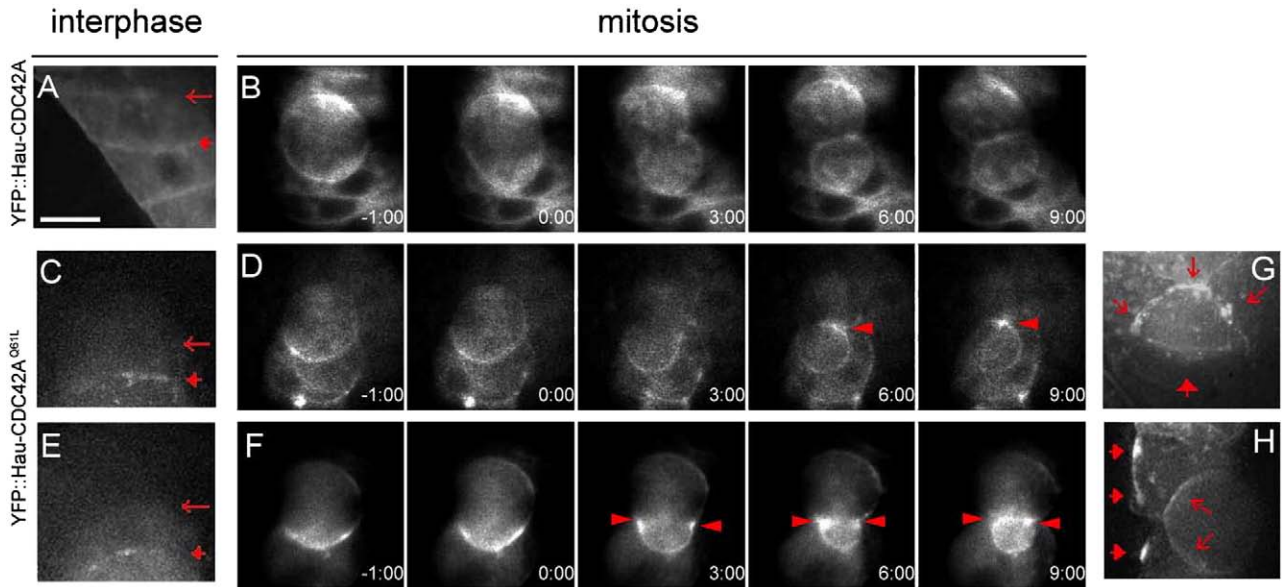


Fig. 7. Localization of YFP fusion proteins. YFP::Hau-CDC42A (A, B) and YFP::Hau-CDC42A^{Q61L} (C–F) in interphase cells (A, C, E) and during mitoses (B, D, F) show selected frames from time-lapse videos; elapsed time indicated in minutes. YFP::Hau-CDC42A localizes to both anterior and posterior cortices (long and short arrows, respectively) of all *n* blast cells. Low levels of YFP::Hau-CDC42A^{Q61L} localize to posterior but not anterior cortices in *ns* (C) and *nf* (E) during interphase, and segregate to the smaller posterior daughter cells in mitosis (D, F). In (B, D, F), gray-scale images were exponentially transformed to enhance differences in fluorescence intensity. Time zero marks the initiation of cytokinesis. Note that the highest YFP intensity was detected at progressing cytokinetic furrows (arrowheads). (G, H) In more posterior cells with higher expression levels, YFP::Hau-CDC42A^{Q61L} localizes to multiple cortical foci (arrows) during interphase (G) and these are inherited by both daughters in the equalized mitoses (H). Scale bar, 10 microns.

Given the short time windows over which time lapse observations could be made, it was not technically feasible to follow the subsequent divisions of affected *n* blast cells in detail. However, in embryos examined about 96 h after injection *yfp::Hau-cdc42a*^{G12V/Q61L}, affected *n* blast cell clones had apparently undergone very few additional, equal divisions. The resultant clones comprised isolated clusters of several equally sized nuclei. In some cases, fragmented nuclei suggested the occurrence of cell death in the affected clones (Fig. 6D), but at least some affected cells were observed to persist, without obvious differentiation, through developmental stage 10, when normally developing segments are well-differentiated (not shown).

Imaging live embryos revealed that the equally dividing *n* blast cells had multiple patches of cortical YFP distributed throughout the cortex (Figs. 7G, H), in contrast to the posteriorly localized signal seen in asymmetrically dividing *n* blast cells expressing low levels of constitutively active YFP::Hau-CDC42A^{G12V/Q61L}. Taken together, these results suggest that Hau-CDC42A activity is normally localized to posterior cortices of *nf* and *ns* blast cells, and that over-expressing the constitutively active form of Hau-CDC42A disrupts *nf* and *ns* asymmetric mitoses once a critical threshold CDC42 activity is exceeded.

Common threshold of *nf* and *ns* in response to CDC42A^{G12V/Q61L} over-expression

Do the normally observed differences in the extent of the asymmetry between *ns* and *nf* blast cell divisions result from quantitative differences in the amounts of activated Hau-CDC42A in the two cell types? If so, we predicted that the nuclear ratios of dividing *n* blast cells would shift gradually from their normal values toward unity, and also that *nf* cells might be more sensitive than *ns* cells to increasing levels of Hau-CDC42A^{G12V/Q61L}. In fact, neither of these predictions was met. In experimental embryos, the transition from asymmetric to symmetric divisions was abrupt, as if the cells respond to increasing CDC42 activity in a switch-like, all or none manner (Figs. 6B, C), and the first affected clone was equally likely to arise from an *ns* or *nf* blast cell (data not shown).

To further test the possibility that quantitative differences in intracellular levels of activated Hau-CDC42A control the differential asymmetry of *nf* and *ns* blast cell divisions, *N* teloblasts were injected with serially diluted *yfp::Hau-cdc42a*^{G12V/Q61L} mRNA, to generate a shallower gradient of increasing YFP::Hau-CDC42A^{G12V/Q61L} expression in the blast cells. As the mRNA concentration in the needle decreased from 0.4 to 0.2 $\mu\text{g}/\mu\text{l}$, the number of blast cells produced before abnormal (equal) divisions began increased to ~ 14 (Fig. 6F), but the transition remained abrupt, with nuclear ratios changing to unity with neither any intermediate values nor with any bias in terms of which cell type was affected first. At lower mRNA concentrations, increasing numbers of *n* blast clones developed normally but there was still an abrupt transition from normal to abnormal development in the clones expressing Hau-CDC42A^{G12V/Q61L} (Figs. 6D, F). We also injected *N* teloblasts at different time during stage 7, thereby targeting primary blast cells at various positions along the A–P axis, with no change in the results. We therefore conclude that a slight increase in the concentrations of Hau-CDC42A^{G12V/Q61L} level above some common threshold value disrupted the normal asymmetry in both *ns* and *nf* blast cells in an “all-or-none” manner. Moreover, all *ns* and *nf* primary blast cells along A–P axis have the same threshold to the effects of Hau-CDC42A^{G12V/Q61L}.

Further evidence for this threshold effect comes from the *N* teloblasts themselves. Teloblasts injected with *yfp::Hau-cdc42a*^{G12V/Q61L} continued making morphologically normal primary blast cells for some time even when the blast cells produced were destined to divide evenly, but in most embryos, the injected teloblast eventually made an approximately equal division and ceased producing primary blast cells (Fig. 6E), truncating that *N* lineage. This suggests that the *N* teloblasts also respond in an all-or-none manner to increasing levels of constitutively active Hau-CDC42A, but with a higher threshold than the primary blast cells.

Discussion

We have shown here that the *cdc42*-class gene, encoding a highly conserved Rho family GTPase, is duplicated in the genome of the leech *Helobdella*. This duplication presumably occurred within the annelid

sub-lineage leading to *Helobdella* after the divergence of the ancestors of *Helobdella*, a clitellate annelid, and *Capitella*, a polychaete annelid, since the latter contains only one *cdc42* homolog (Fig. 2).

We also find that one of the two genes, CDC42A, is differentially expressed between the two classes of alternating blast cells (higher in ns and lower in nf blast cells) arising in the N teloblast lineage, a grandparental stem cell lineage which generates most of the segmental central nervous system in leeches and other clitellate annelids (Figs. 1, 4). Differences in *Hau-cdc42a* mRNA levels in ns and nf segmental founder cells are evident by about 6 h clonal age, but translation of *Hro-cdc42a* is repressed for about 20 h after this time (Fig. 4). The eponymous grandparental stem cell iteration (Chalfie et al., 1981) arises as an aberrant lineage in *C. elegans* lin-4 microRNA mutants (Lee et al., 2004), but no involvement of Rho GTPases has been reported for this process. Thus, at this point, we assume that the similarities between the grandparental stem cell lineages in *Helobdella* and *Caenorhabditis* are purely operational, and do not reflect a common molecular mechanism.

Cdc42 and the cell biology of polarized cell division

In our experiments, YFP::Hau-CDC42A was enriched at both the anterior and posterior cell cortices, relative to the lateral cortices; over-expressing this protein did not perturb cell division patterns. In contrast, low levels of the constitutively active form of the protein localized to the posterior cortex, suggesting that the activated, GTP-bound form of Cdc42A is preferentially recruited to a site at the posterior cortex of both nf and ns blast cells. Higher levels of constitutively active YFP::Cdc42A led to the appearance of ectopic protein foci and to the equalization of n blast cell divisions (Fig. 7). Finally, it appears that ns and nf cells have the same threshold for constitutively active Hau-CDC42A despite their differences in overall Hau-CDC42A levels. From this, we conclude that a smaller fraction of the overall Hau-CDC42A is activated and localized in ns cells than in nf cells.

Differential localization of Cdc42 activity is a widely conserved feature of cell polarity and asymmetric cell division, but the presently known details of the mechanisms and its developmental consequences vary from one biological context to another. For example, during polar body formation in mouse oocyte, activated Cdc42 is localized to the cortex contained within the prospective contractile ring defined by RhoA; thus the distribution of activated Cdc42 defines the cortex of the nascent polar body (Zhang et al., 2008), analogous to the association of activated Hau-CDC42A with the prospective smaller, posterior daughters of the n blast cell divisions. Expression of either dominant negative or constitutively active forms of Cdc42 in the mouse oocyte symmetrizes the meiotic spindle, so that both ends approach the cortex on opposite sides of the cell, though these cells fail to divide (Na and Zernicka-Goetz, 2006). In the radial polarization of the *C. elegans* embryo, a critical step is the localization of a Rho GTPase activating protein (GAP) to the basolateral cortices of the blastomeres. GAP activity inactivates Cdc42 in basolateral territory, thereby restricting the activated (GTP bound) form of Cdc42 to the apical cortex, where it recruits PAR6 and thence the other components of the PAR3/PAR6/aPKC complex (Anderson et al., 2008). Yet another example of Cdc42 activity is provided by cultured cells of a human intestinal epithelial line (Caco-2 cells), which generate cyst-like structures when grown in a 3-D matrix; in contrast to the situation with *C. elegans* blastomere polarization, depletion of Cdc42 in Caco-2 cells disrupts spindle orientation during mitosis without affecting the apical-basal polarity of the epithelial cells (Jaffe et al., 2008). Finally, an apparent exception to the requirement for differential localization of activated Cdc42 in asymmetric cell divisions, in the polarized divisions of *Drosophila* neuroblasts, turned out not to be so; expressing constitutively active Cdc42 under the control of an early acting promoter leads to a broader distribution of

the Par-6/aPKC complex and equalization of the neuroblast divisions (Atwood et al., 2007).

Our finding that tracer levels of constitutively active YFP::Hau-CDC42A^{G12V/Q61L} exhibit a polarized localization not seen with the comparable wild-type fusion protein (Fig. 7) was an unexpected result. In budding yeast, for example, wild type Cdc42 protein becomes enriched at the prospective bud site prior to bud formation (Ziman et al., 1993; Richman et al., 2002). Other experiments showed that the Cdc42-activating GEF (Cdc24) is also pre-localized to the bud site by binding to proteins associated with the scar from the previous bud (Toenjes et al., 1999); this latter observation accounts for the localization of Cdc42 activity, but does not suffice to explain the localization of bulk Cdc42 protein. One possibility is that Cdc42 is bound to the bud site by other factors associated with the bud site and then activated by Cdc24; if so, Cdc42 localization should proceed normally in mutant cells containing inactive Cdc24. Another possibility is that only the activated (GTP bound) form of Cdc42 is localized to the bud site; in this case, constitutively active Cdc42^{Q61L} should still localize to the bud site in the absence of Cdc24/GEF activity whereas wildtype Cdc42 would fail to localize. To our knowledge, this experiment has not been done.

A third possibility is that the localization and activation of Cdc42 proceeds by a positive feedback mechanism, in which localization and activation of Cdc42 are self-reinforcing so that neither process is strictly upstream of the other (Wedlich-Soldner et al., 2003). A modeling study has shown that a feedback process could lead to the formation of stochastically determined aggregations of Cdc42 even in an initially non-polarized cell. One critical parameter of this model is N, the number of activated Cdc42 molecules in the cell. Consistent with our work using the leech n blast cells, the model predicts that as the number of activated Cdc42 molecules increases, a point is reached at which their distribution becomes homogeneous and the cell fails to polarize.

In any case, our results show that the distribution of wild type Cdc42 protein does not reveal the focus of its activity in this metazoan embryo, in contrast to the situation in yeast, where wild type and activated Cdc42 show the same distribution at the future bud site (Ziman et al., 1993). Thus, the approach introduced here, observing the distribution of low levels of constitutively active Cdc42 to infer the site of action of activated Cdc42 within the cell, may be of use in resolving questions regarding the role of Cdc42 proteins in cell polarization and asymmetric divisions in other systems.

Grandparental stem cell lineages in segmentation

The alternation of ns and nf blast cell fates in the N lineage and the autonomous development of their respective clones are fundamental to the development of the segmented central nervous system of the leech (Shain et al., 2000). Moreover, the question of when and how ns and nf become different from each other is also of interest because it bears on our understanding of how segmentation has evolved among the protostomes. For example, prior to the formulation of the Lophotrochozoa-Ecdysozoa Hypothesis for protostome phylogeny (Aguinaldo et al., 1997), it was generally believed that the last common ancestor of annelids and arthropods was already segmented. At that time, we postulated that the grandparental stem cell lineages in leech might employ homologs of *Drosophila* segmentation genes to generate the distinct nf and ns fates.

However, studies of several leech homologs of *Drosophila* segment polarity and pair rule genes failed to reveal any early molecular differences between nf and ns blast cells (Kostriken and Weisblat, 1992; Lans et al., 1993; Kang et al., 2003; Song et al., 2002, 2004), and the question of how the nf and ns cells assume their distinct fates has remained open. Moreover, so far as is known, there is no grandparental stem cell patterning among arthropods that exhibit teloblastic segmentation, so this may be a derived trait seen only in annelids,

perhaps only in clitellate annelids. Clitellate annelids (oligochaetes and leeches) are a monophyletic group (Erseus and Kallersjo, 2004). Teloblastic lineage patterns homologous to those known for the N teloblasts in leech have been described for oligochaetes, including *Tubifex* and *Eisenia* (Storey, 1989; Arai et al., 2001), as well as in leeches, so it seems likely that this feature is ancestral to the clitellates. Beyond the clitellates, annelid phylogeny is not well resolved. But given the conservation of cleavage patterns between clitellates and some polychaete groups (Dohle, 1999), it may be that grandparental stem cell lineages will be found among polychaetes as well. Should it turn out that the grandparental mode of stem cell division is a unique and ancestral feature of annelid segmentation, it would suggest the possibility that segmentation in annelids and arthropods are fundamentally different processes, consistent with the idea that segmentation evolved independently in these two proto-stome groups.

Previous studies showed differences in the composition of alternate cell cycles in the N teloblasts (Bissen and Weisblat, 1987), leading us to postulate that ns and nf blast cells are assigned distinct identities at birth by an oscillator of two-cell cycle periodicity operating in the parent teloblast (Weisblat et al., 1994). Somewhat contrary to this hypothesis, however, our finding that the final pattern of *Hau-cdc42a* levels is established only several hours after the n blast cells are born (Fig. 4) suggests that at least some aspects of the distinct ns and nf cell identities are not assigned by the parent teloblast, but instead arise by interactions of n blast cells among themselves or with their environment.

We were frustrated in our attempts to uncover a functional significance for the presumed difference in *Hau-CDC42A* levels between ns and nf blast cells. In any event, finding that *Hau-cdc42a* expression varies systematically between the two alternating classes of n blast cells provides an entry point for studying the mechanism by which these differences are established, and thus provides the first insights into an apparently novel process in which two cell types arise from one stem cell lineage.

Acknowledgments

We thank Drs. Gian Garriga, John Gerhart and Bob Goldstein for comments on this paper. This work is supported by NIH grant RO1 GM60240 to D.A.W.

References

- Agee, S.J., Lyons, D.C., Weisblat, D.A., 2006. Maternal expression of a NANOS homolog is required for early development of the leech *Helobdella robusta*. *Dev. Biol.* 298, 1–11.
- Aguinaldo, A.M.A., Turbeville, J.M., Linford, L.S., Rivera, M.C., Garett, J.R., Raff, R.A., Lake, J.A., 1997. Evidence for a clade of nematodes, arthropods and other moulting animals. *Nature* 387, 489–493.
- Anderson, D.C., Gill, J.S., Cinalli, R.M., Nance, J., 2008. Polarization of the *C. elegans* embryo by RhoGAP-mediated exclusion of PAR-6 from cell contacts. *Science* 320, 1771–1774.
- Arai, A., Nakamoto, A., Shimizu, T., 2001. Specification of ectodermal teloblast lineages in embryos of the oligochaete annelid *Tubifex*: involvement of novel cell-cell interactions. *Development* 128, 1211–1219.
- Atwood, S.X., Chabu, C., Penkert, R.R., Doe, C.Q., Prehoda, K.E., 2007. Cdc42 acts downstream of Bazooka to regulate neuroblast polarity through Par-6 aPKC. *J. Cell Sci.* 120, 3200–3206.
- Bely, A.E., Weisblat, D.A., 2006. Lessons from leeches: a call for DNA barcoding in the lab. *Evol. Dev.* 8, 491–501.
- Bissen, S.T., Weisblat, D.A., 1987. Early differences between alternate n blast cells in leech embryo. *J. Neurobiol.* 18, 251–270.
- Boureux, A., Vignal, E., Faure, S., Fort, P., 2007. Evolution of the Rho family of ras-like GTPases in eukaryotes. *Mol. Biol. Evol.* 24, 203–216.
- Chalfie, M., Horvitz, H.R., Sulston, J.E., 1981. Mutations that lead to reiterations in the cell lineages of *C. elegans*. *Cell* 24, 59–69.
- Dohle, W., 1999. The ancestral cleavage pattern of the clitellates and its phylogenetic deviations. *Hydrobiologia* 402, 267–283.
- Erseus, C., Kallersjo, M., 2004. 18S rDNA phylogeny of Clitellata (Annelida). *Zool. Scr.* 33, 187–196.
- Etienne-Manneville, S., Hall, A., 2002. Rho GTPases in cell biology. *Nature* 420, 629–633.
- Gimlich, R.L., Braun, J., 1985. Improved fluorescent compounds for tracing cell lineage. *Dev. Biol.* 109, 509–514.
- Goldstein, B., Leviten, M.W., Weisblat, D.A., 2001. Dorsal and Snail homologs in leech development. *Dev. Genes Evol.* 211, 329–337.
- Guindon, S., Lethiec, F., Duroux, P., Gascuel, O., 2005. PHYML online—a web server for fast maximum likelihood-based phylogenetic inference. *Nucleic Acids Res.* 33, W557–W559.
- Hall, A., 2005. Rho GTPases and the control of cell behaviour. *Biochem. Soc. Trans.* 33, 891–895.
- Hutterer, A., Betschinger, J., Petronczki, M., Knoblich, J.A., 2004. Sequential roles of Cdc42, Par-6, aPKC, and Lgl in the establishment of epithelial polarity during *Drosophila* embryogenesis. *Dev. Cell* 6, 845–854.
- Jaffe, A.B., Kaji, N., Durgan, J., Hall, A., 2008. Cdc42 controls spindle orientation to position the apical surface during epithelial morphogenesis. *J. Cell Biol.* 183, 625–633.
- Kang, D., Huang, F., Li, D., Shankland, M., Gaffield, W., Weisblat, D.A., 2003. A hedgehog homolog regulates gut formation in leech (*Helobdella*). *Development* 130, 1645–1657.
- Kostriken, R., Weisblat, D.A., 1992. Expression of a *Wnt* gene in embryonic epithelium of the leech. *Dev. Biol.* 151, 225–241.
- Kuo, D.-H., Shankland, M., 2004. Evolutionary diversification of specification mechanisms within the O/P equivalence group of the leech genus *Helobdella*. *Development* 131, 5859–5869.
- Lans, D., Wedeen, C.J., Weisblat, D.A., 1993. Cell lineage analysis of the expression of an engrailed homolog in leech embryos. *Development* 117, 857–871.
- Larkin, M.A., Blackshields, G., Brown, N.P., Chenna, R., McGettigan, P.A., McWilliam, H., Valentin, F., Wallace, I.M., Wilm, A., Lopez, R., Thompson, J.D., Gibson, T.J., Higgins, D.G., 2007. Clustal W and Clustal X version 2.0. *Bioinformatics* 23, 2947–2948.
- Lee, R., Feinbaum, R., Ambros, V., 2004. A short history of a short RNA. *Cell* 116 (Suppl.), S89–S92.
- Na, J., Zernicka-Goetz, M., 2006. Asymmetric positioning and organization of the meiotic spindle of mouse oocytes requires CDC42 function. *Curr. Biol.* 16, 1249–1254.
- Ren, X., Weisblat, D.A., 2006. Asymmetrization of first cleavage by transient disassembly of one spindle pole aster in the leech *Helobdella robusta*. *Dev. Biol.* 292, 103–115.
- Richman, T.J., Sawyer, M.M., Johnson, D.I., 2002. *Saccharomyces cerevisiae* Cdc42p localizes to cellular membranes and clusters at sites of polarized growth. *Eukaryot. Cell* 1, 458–468.
- Seaver, E.C., Shankland, M., 2000. Leech segmental repeats develop normally in the absence of signals from either anterior or posterior segments. *Dev. Biol.* 224, 339–353.
- Seaver, E.C., Shankland, M., 2001. Establishment of segment polarity in the ectoderm of the leech *Helobdella*. *Development* 128, 1629–1641.
- Shain, D.H., Stuart, D.K., Huang, F.Z., Weisblat, D.A., 2000. Segmentation of the central nervous system in leech. *Development* 127, 735–744.
- Shankland, M., Bissen, S.T., Weisblat, D.A., 1992. Description of the Californian leech *Helobdella robusta* sp. nov. and comparison with *Helobdella triserialis* on the basis of morphology, embryology and experimental breeding. *Can. J. Zool.* 70, 1258–1263.
- Song, M.H., Huang, F.Z., Chang, G.Y., Weisblat, D.A., 2002. Expression and function of an even-skipped homolog in the leech *Helobdella robusta*. *Development* 129, 3681–3692.
- Song, M.H., Huang, F.Z., Gonsalves, F.C., Weisblat, D.A., 2004. Cell cycle-dependent expression of a hairy and Enhancer of split (*hes*) homolog during cleavage and segmentation in leech embryos. *Dev. Biol.* 269, 183–195.
- Storey, K.G., 1989. Cell lineage and pattern formation in the earthworm embryo. *Development* 107, 519–532.
- Takai, Y., Sasaki, T., Matozaki, T., 2001. Small GTP-binding proteins. *Physiol. Rev.* 81, 153–208.
- Tamara, K., Dudley, J., Nei, M., Kumar, S., 2007. MEGA4: Molecular Evolutionary Genetics Analysis (MEGA) software version 4.0. *Mol. Biol. Evol.* 24, 1596–1599.
- Toenjes, K.A., Sawyer, M.M., Johnson, D.I., 1999. The guanine-nucleotide-exchange factor Cdc24p is targeted to the nucleus and polarized growth sites. *Curr. Biol.* 9, 1183–1186.
- Wedlich-Soldner, R., Altschuler, S., Wu, L., Li, R., 2003. Spontaneous cell polarization through actomyosin-based delivery of the Cdc42 GTPase. *Science* 299, 1231–1235.
- Weisblat, D.A., Huang, F.Z., 2001. An overview of glossiphoniid leech development. *Can. J. Zool.* 79, 218–232.
- Weisblat, D.A., Shankland, M., 1985. Cell lineage and segmentation in the leech. *Philos. Trans. R. Soc. Lond., B* 312, 39–56.
- Weisblat, D.A., Wedeen, C.J., Kostriken, R.G., 1994. Evolution of developmental mechanisms: spatial and temporal modes of rostrocaudal patterning. *Curr. Top. Dev. Biol.* 29, 101–134.
- Zackson, S.L., 1984. Cell lineage, cell-cell interaction, and segment formation in the ectoderm of a glossiphoniid leech embryo. *Dev. Biol.* 104, 143–160.
- Zhang, S.O., Weisblat, D.A., 2005. Applications of mRNA injections for analyzing cell lineage and asymmetric cell divisions during segmentation in the leech *Helobdella robusta*. *Development* 132, 2103–2113.
- Zhang, X., Ma, C., Miller, A.L., Arabi Katbi, H., Bement, W.M., Liu, X.J., 2008. Polar body emission requires a RhoA contractile ring and Cdc42-mediated membrane protrusion. *Dev. Cell* 15, 386–400.
- Ziman, M., Preuss, D., Mulholland, J., O'Brien, J.M., Botstein, D., Johnson, D.I., 1993. Subcellular localization of Cdc42p, a *Saccharomyces cerevisiae* GTP-binding protein involved in the control of cell polarity. *Mol. Biol. Cell* 4, 1307–1316.